Pure Appl. Geophys. 174 (2017), 1425–1440
© 2017 Springer International Publishing
DOI 10.1007/s00024-017-1474-5

Pure and Applied Geophysics

The Stress/Strain Analysis of Kinematic Structure at Gülbahçe Fault and Uzunkuyu Intrusive (İzmir, Turkey)

Ayça Çırmık,[1] Fikret Doğru,[1] Tolga Gönenç,[1] and Oya Pamukçu[1]

Abstract—İzmir and its surroundings constitute an important tectonic region for the control of the Western Anatolian region. The study area is located in the western part of İzmir city and inside of Karaburun Peninsula. In the study area and its surroundings, a great amount of earthquakes occurred in both land and sea in recent years. Hence, the kinematic structures of Gülbahçe fault and Uzunkuyu intrusive were examined within this study. As a first step, the mechanism and the velocities of these faults were identified using the GNSS data. Then, a stress and strain analysis of the region was performed for different depths using Coulomb software. In this study, the strain changes on vertical direction were evaluated and compared with the changes of observed gravity anomalies for the first time for the study area as distinct from the previous studies. From this integrated analysis, we retrieved the kinematic parameters and movement mechanisms of Gülbahçe fault and Uzunkuyu intrusive and defined the regional stresses, the strain changes and the kinematic models of them.

Key words: Gülbahçe fault, Uzunkuyu intrusive, Karaburun Peninsula, stress/strain analysis, GNSS, gravity.

1. Introduction

The study area is located in the western side of İzmir city, in Karaburun Peninsula extending throughout Aegean Sea (Fig. 1). Aegean Sea and Western Anatolia have a complex tectonism within N–S oriented extension (McKenzie 1972; Dewey and Şengör 1979). Gulf of İzmir shows NNW–SSE directional extension with the effect of E–W oriented basins of Western Anatolia. Additionally, the N–NE oriented blocks, oblique faults and E–W oriented normal faults have shaped Gulf of İzmir (Kaya 1979, 1981). The previous studies (Saroglu et al. 1992; Emre and Barka 2000; Altunkaynak and Yılmaz 2000; Genç et al. 2001) pointed out that there are some active N–S to NE–SW oriented strike-slip faults in the study area and besides, Karaburun Fault (Emre et al. 2005), Gülbahçe Fault (Emre et al. 2005) and Karaburun Seismic Zone (KSZ) (Tan 2013) are identified as the main tectonic structures of the study area. In the studies of Pamukçu et al. (2015a, b) conducted in southward of İzmir and in Sığacık bay, it was pointed out that the seismically active area including surroundings of Gülbahçe fault are very complicated and this area should be studied in detail.

Gülbahçe fault is a significant line which structurally and morphologically separates Gulf of İzmir and Karaburun Peninsula. The length of the onland part of Gülbahçe fault is 15 km along Gülbahçe Bay on the north and Sığacık Bay on the south. Both ends of the N–S oriented fault are located under the sea. The total length of the fault is approximately 70 km by considering the submarine parts (Emre et al. 2005).

The onland studies evidenced that Gülbahçe fault controls the Quaternary morphology. The submarine studies provided clearer data about the properties of the fault and its effectiveness in Quaternary age (Ocakoğlu et al. 2004, 2005; Aksu et al. 1987). The northward continuity of Gülbahçe fault which lies throughout the basement of Gulf of İzmir and the geometrical relation of this fault with the other faults has not been interpreted clearly (Emre et al. 2005). According to the seismic study of Ocakoğlu et al. (2005), the orientation of the fault, which is N–S on Gülbahçe Bay, turns to NNW–SSE in the north and there are lots of parallel faults to that fault at offshore Karaburun, besides, most of these faults have inverse dip-slip segments.

[1] Department of Geophysical Engineering, Engineering Faculty, Dokuz Eylul University, 35160 Izmir, Turkey. E-mail: oya.pamukcu@deu.edu.tr

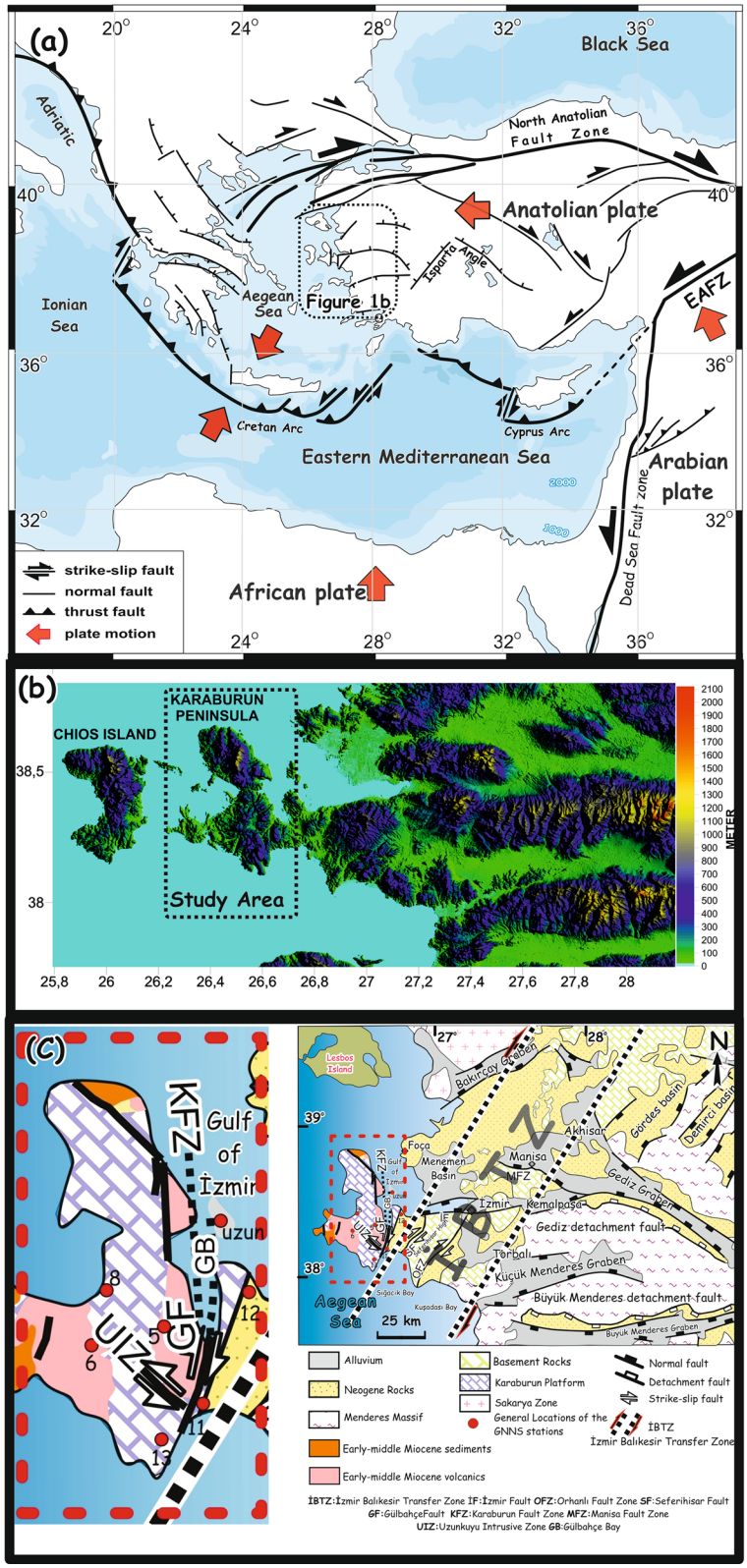
(a)
Black Sea
Adriatic
North Anatolian Fault Zone
Anatolian plate
Ionian Sea
Aegean Sea
Figure 1b
Isparta Angle
EAFZ
Cretan Arc
Cyprus Arc
Eastern Mediterranean Sea
Arabian plate
Dead Sea Fault zone
African plate
strike-slip fault
normal fault
thrust fault
plate motion
(b)
KARABURUN PENINSULA
CHIOS ISLAND
Study Area
METER
(C)
KFZ
Gulf of İzmir
GB
uzun
GF
UIZ
Lesbos Island
Bakırçay Graben
Foça
Menemen Basin
Manisa
MFZ
Akhisar
Gördes basin
Demirci basin
İzmir
Kemalpaşa
Gediz Graben
Gediz detachment fault
Torbalı
Küçük Menderes Graben
Büyük Menderes detachment fault
Aegean Sea
25 km
Alluvium
Neogene Rocks
Menderes Massif
Early-middle Miocene sediments
Early-middle Miocene volcanics
Basement Rocks
Karaburun Platform
Sakarya Zone
General Locations of the GNNS stations
Normal fault
Detachment fault
Strike-slip fault
İBTZ
İzmir Balıkesir Transfer Zone
İBTZ:İzmir Balıkesir Transfer Zone IF:İzmir Fault OFZ:Orhanlı Fault Zone SF:Seferihisar Fault
GF:GülbahçeFault KFZ:Karaburun Fault Zone MFZ:Manisa Fault Zone
UIZ:Uzunkuyu Intrusive Zone GB:Gülbahçe Bay

◀Figure 1
a The main geological characteristics of Western Anatolia (redrawn from Taymaz et al. 2007 and compiled from Şengor et al. 1985; Barka 1992; Bozkurt 2001; Kocyigit and Özacar 2003; Kaymakcı et al. 2007; Uzel et al. 2012. EAFZ—East Anatolian Fault Zone. Heavy lines with half arrows are strike-slip faults with *arrows* showing relative movement sense. **b** General morphology of study area. **c** Simplified geological map depicting main basins on Gulf of İzmir and the surroundings with the study area (Kaya 1981; Bozkurt 2001; Emre et al. 2005; Pamukçu et al. 2014; Uzel and Sözbilir 2008; Uzel et al. 2012, 2015)

Gülbahçe fault is established as the significant earthquake source for İzmir and its surroundings. The geometrical segments of the fault which have importance for earthquake risk analysis have not been defined in detail since the greatest part of the fault locates under the sea. The findings concluded that the dominant mechanism on Gülbahçe fault is the strike-slip. However, the direction of the strike-slip in Holocene could not be determined (Emre et al. 2005). The submarine data explained that the inverse segment exists along the northern segment of the fault and the western block has been pushed onto the eastern block (Ocakoğlu et al. 2005). Some onland studies pointed out that the surface of the Karaburun block is tilted westwards and this observation is coherent with the existence of inverse segment suggested in the study of Ocakoğlu et al. (2005). The regional morphotectonical structure and the compressional segment monitored along the northern segment of the fault in the general fault geometry suggested that the sense of the fault can be right-lateral strike slip (Emre et al. 2005).

Tan (2013) defined a seismic zone in the west of İzmir city, namely, the Karaburun seismic zone (KSZ). According to Tan (2013), the 40 km-long zone is NW–SE oriented with a left-lateral strike–slip movement and originates high micro-earthquake activity. The study area is worthy of being further studied in detail, for the presence of another, significant tectonic structure, the Uzunkuyu intrusive, which is located in the middle of KSZ.

In this study, the GNSS data of the Scientific and Technological Research Council of Turkey (TUBITAK) project realized between the years 2009 and 2011 in the area including Gülbahçe fault and Uzunkuyu intrusive were processed and the relative solutions were evaluated with respect to the faults using the GAMIT/GLOBK (GG) software (Herring et al. 2010a, b; King and Bock 2009). Then, the obtained GNSS velocities were modelled with fault parameters using Coulomb 3.3 software (Toda et al. 2005; Lin and Stein 2004). The stresses and strains of the models were analyzed with the values calculated by Coulomb 3.3 software. As the final step, the observed gravity data of the study area were compared with the vertical component of the strain values.

Consequently, in this study the features of two significant tectonic structures; Gülbahçe fault and Uzunkuyu intrusive, which control the seismic activity of the study area, were analyzed in detail. Therefore, this study provides a significant contribution to the literature with detailed investigations.

2. Data Analysis

In this study, as first step, we calculated GNSS velocities relative to Gülbahçe fault and Uzunkuyu intrusive. As second step, we modelled Gülbahçe fault and Uzunkuyu intrusive and obtained the stress–strain values. At the last step, we evaluated the tectonic borders of these structures with the Bouguer gravity anomalies.

2.1. Relative Solutions of GNSS Data

The main tectonic structures of the study area are Gülbahçe fault and Uzunkuyu intrusive (Fig. 1) or the Karaburun seismic zone which was defined by Tan (2013). For investigating these elements, the GNSS data measured in 2009, 2010 and 2011 in TUBITAK project were processed with respect to a fixed Eurasian plate in ITRF-2008 (International Terrestrial Reference Frame) using GG. Therefore, 10 IGS (International GNSS Service) stations; TUBI, ISTA, ZECK, NICO, MIKL, GLSV, BUCU, PENC, WTZR and MATE were used for defining the coordinates and velocities of GNSS stations. Then, the relative solutions were calculated for determining the kinematic structures of Gülbahçe fault and Uzunkuyu intrusive. In this step, the relative motions of the stations located on opposite sides of a boundary were calculated using GG. In this

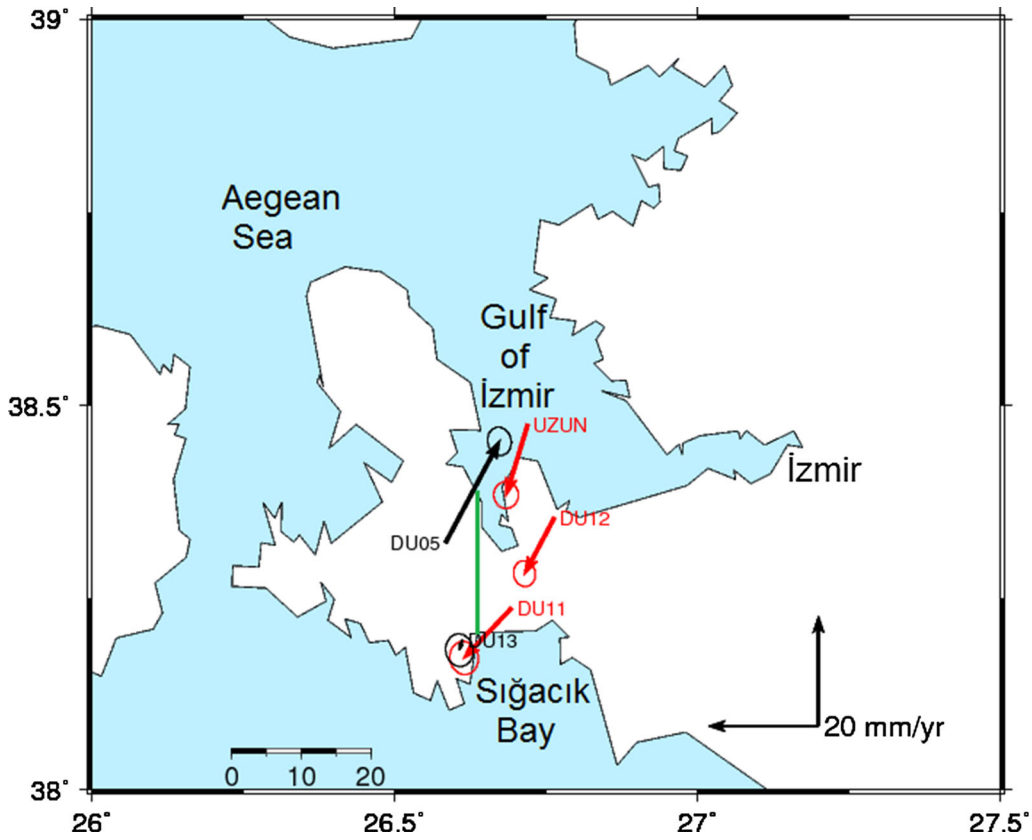

Figure 2
The relative solutions of GNSS stations located around Gülbahçe fault. *Green line* represents Gülbahçe fault

calculation, while obtaining the velocities of the stations located on one side, the opposite side stations are assumed as stable (their motions are zero). As first step, the GNSS stations; DU05, DU11, DU12, DU13 and UZUN (Fig. 2) were used for defining the relative solutions related to the Gülbahçe fault, UZUN, DU11 and DU12 were chosen as right side and DU05, DU13 were chosen as left side stations. The GNSS velocities of right side stations (UZUN, DU11 and DU12) were calculated relative to left side stations (by assuming the motions of left side stations are zero), then, GNSS velocities of left side stations (DU05 and DU13) were calculated relative to the opposite side stations (by assuming the movements of right side stations are zero) (Fig. 2). Due to these relative solutions, it was confirmed that the sense of Gülbahçe fault is right-lateral strike slip. However, no solution was obtained for DU13. Therefore, it could be suggested that DU13 is controlled by another kinematic structure.

As second step, DU05, DU06, DU08 and DU13 were used (Fig. 3) for defining the relative solutions related to the Uzunkuyu intrusive. Using the same approach as above, that mechanism was determined as left-lateral strike slip. DU13, which was concluded to be not related to Gülbahçe fault, gave a solution compatible with the activity of Uzunkuyu intrusive (Fig. 3). Moreover, Fig. 3 shows that DU05 velocity is not completely in agreement with the activity of Uzunkuyu intrusive.

2.2. *Coulomb Stress and Strain Analysis*

Coulomb 3.3 is a software used for providing the stresses and strains at any depth. The Coulomb stress change depends on the fault geometry, sense of slip and the coefficient of friction; on the other hand it is independent of regional stress (King et al. 1994). In the Coulomb criterion, if the Coulomb stress σ_f exceeds a specific value, the failure on a plane is given as;

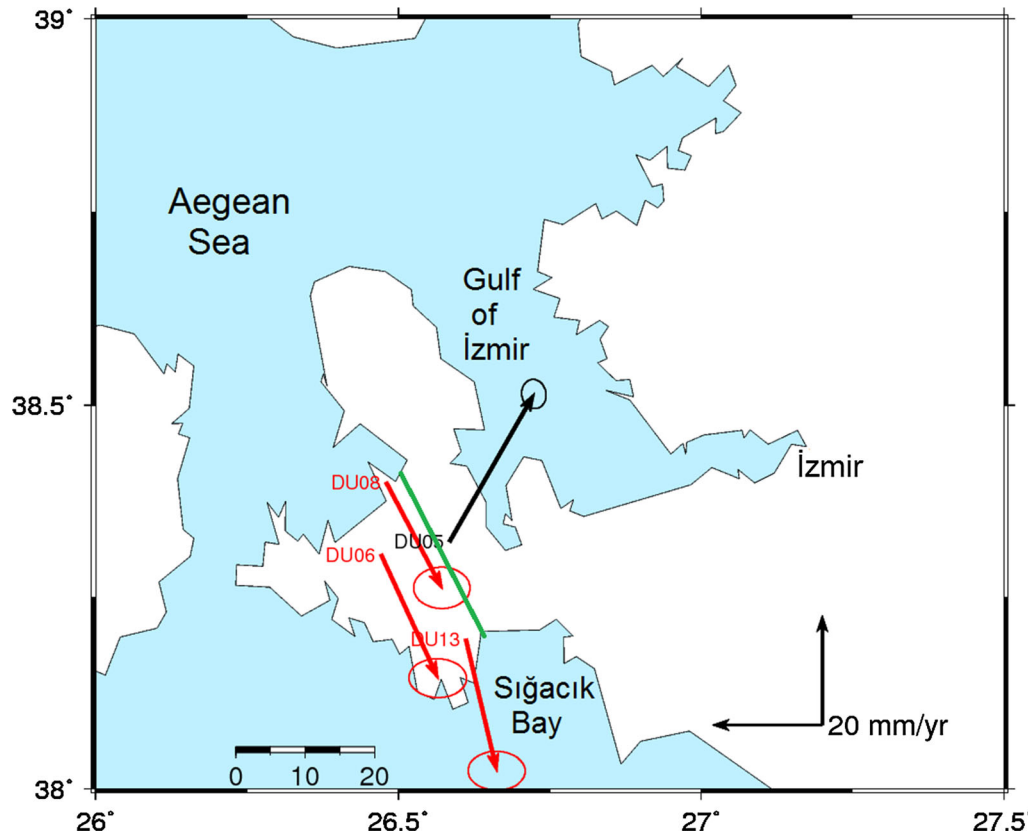

Figure 3
The relative solutions of GNSS stations located around Uzunkuyu intrusive and its surrounding. *Green line* represents Uzunkuyu intrusive

$$\sigma_f = \tau_\beta - \mu(\sigma_\beta - p). \quad (1)$$

Here τ_β is the shear stress on the failure plane, σ_β is the normal stress, μ is the coefficient of friction and p is the pore fluid pressure (King et al. 1994).

If the failure plane is directed at β to the σ_1 axes, the components of the stress can be defined as principal stresses:

$$\sigma_\beta = \frac{1}{2}(\sigma_1 + \sigma_3) - \frac{1}{2}(\sigma_1 - \sigma_3)\cos 2\beta, \quad (2)$$

$$\tau_\beta = \frac{1}{2}(\sigma_1 - \sigma_3)\sin 2\beta, \quad (3)$$

Here, σ_1 is the greatest, σ_3 is the smallest principal stress. Therefore, Eq. 1 becomes;

$$\sigma_f = \frac{1}{2}(\sigma_1 - \sigma_3)(\sin 2\beta - \mu\cos 2\beta) - \frac{1}{2}\mu(\sigma_1 + \sigma_3) + \mu p. \quad (4)$$

If the fault displacements are in the horizontal direction (x and y axes)and the fault planes are in the vertical direction (along z direction), the stress on a plane at an angle σ from the x-axis is given as (King et al. 1994),

$$\sigma_{11} = \sigma_{xx}\cos^2\psi + 2\sigma_{xy}\sin\psi\cos\psi + \sigma_{yy}\sin^2\psi,$$

$$\sigma_{33} = \sigma_{xx}\sin^2\psi + 2\sigma_{xy}\sin\psi\cos\psi + \sigma_{yy}\cos^2\psi,$$

$$\tau_{13} = \frac{1}{2}(\sigma_{yy} - \sigma_{xx})\sin 2\psi + \tau_{xy}\cos 2\psi. \quad (5)$$

In this step, we modelled Gülbahçe fault and Uzunkuyu intrusive with Coulomb 3.3 software using the obtained relative GNSS solutions and then, we calculated the stress and strain values using these models.

First, Gülbahçe fault was modelled (Fig. 4) using the GNSS relative solutions of this fault (Fig. 2). As the result of the modelling, we can conclude that the

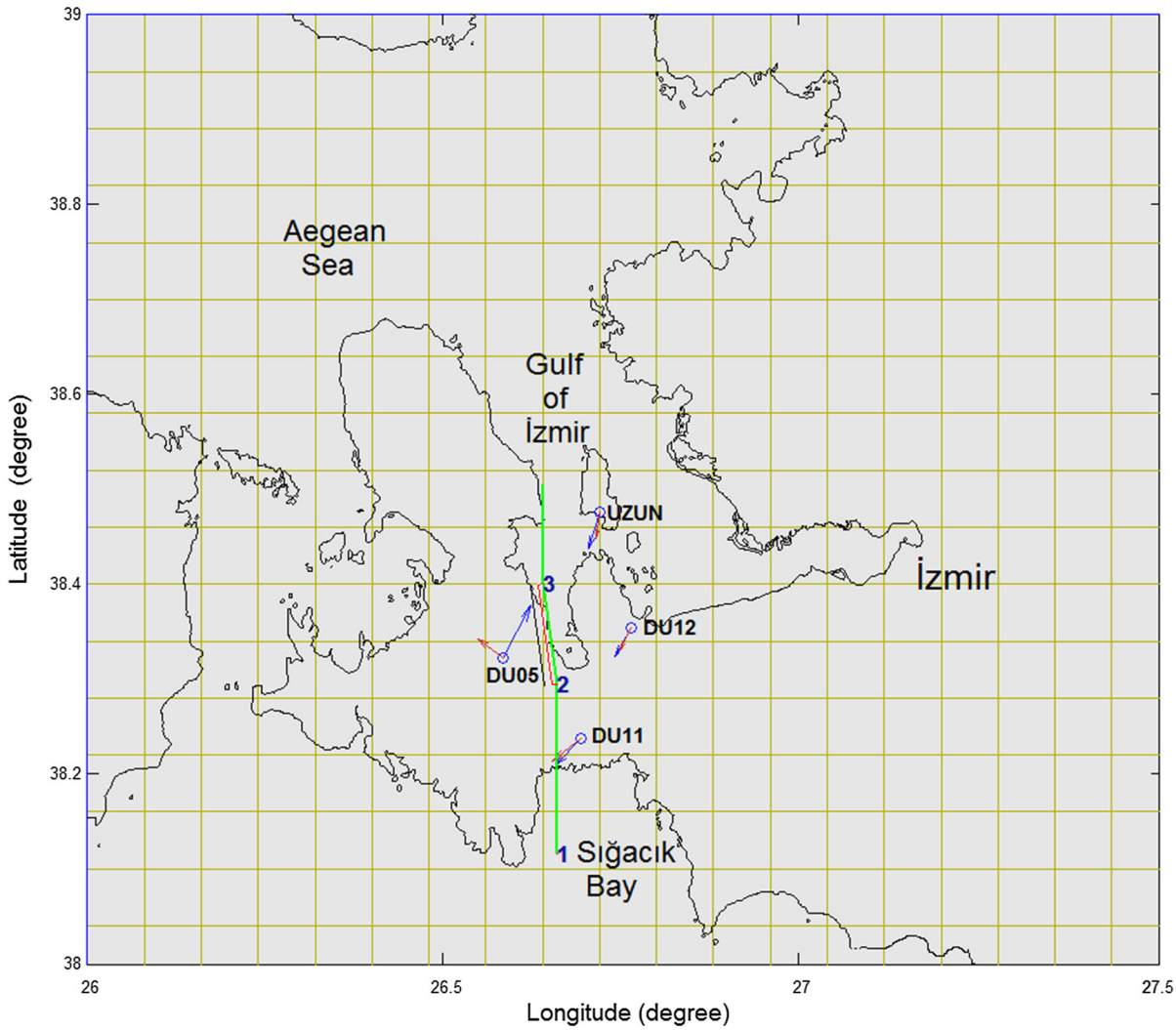

Figure 4
The model created using GNSS relative solutions of Gülbahçe fault. *Blue vectors* represent the obtained GNSS velocities by GG and *red vectors* represent modelled GNSS velocities by Coulomb 3.3. No: 1, 2 and 3 represent the fault segments

fault consists of three segments (Fig. 4). These are: (1) right-lateral strike slip fault, (2) right-lateral strike slip fault, (3) right-lateral reverse oblique fault. The obtained fault parameters (rake, net slip, dip angle and the top and bottom depths of the fault) are given at Table 1.

In Fig. 4, it is seen that DU05 is not coherent with that modelling. Furthermore, the GNSS relative solutions of Gülbahçe fault (Fig. 2) indicated that DU13 is not affected by the kinematic structure of this fault. Therefore, due to the mismatches in this modelling, we generated another model by adding the GNSS relative solutions of Uzunkuyu intrusive (Fig. 5).

In the second model (Fig. 5) five segments were determined. These are: (1) left-lateral strike slip fault, (2) left-lateral strike slip fault, (3) right-lateral reverse oblique fault, (4) right-lateral reverse oblique fault, (5) right-lateral reverse oblique fault. The obtained fault parameters (rake, net slip, dip angle and the top and bottom depths of the fault) are given in Table 1.

In the next step, Coulomb stress changes (Fig. 6) were calculated for the depths between 1 and 8 km using the model given in Fig. 5. In Fig. 6, it appears

Table 1

Coulomb modelling results calculated using GNSS relative solutions of Gülbahçe fault and Uzunkuyu Intrusive

Parameters	Rake (°)	Net slip	Dip angle (°)	Top (km)	Bottom (km)
Segments of Gülbahçe fault (Fig. 4)					
1	−120	0.45	90	0.0	4.0
2	−100	0.80	95	0.0	4.0
3	155	1.00	90	0.0	4.0
Segments of Gülbahçe fault and Uzunkuyu intrusive (Fig. 5)					
1	−18	1.2	85	0.0	4.0
2	−18	1	85	0.0	4.0
3	140	0.6	95	0.0	4.0
4	−130	1	95	0.0	4.0
5	160	1.3	95	0.0	4.0

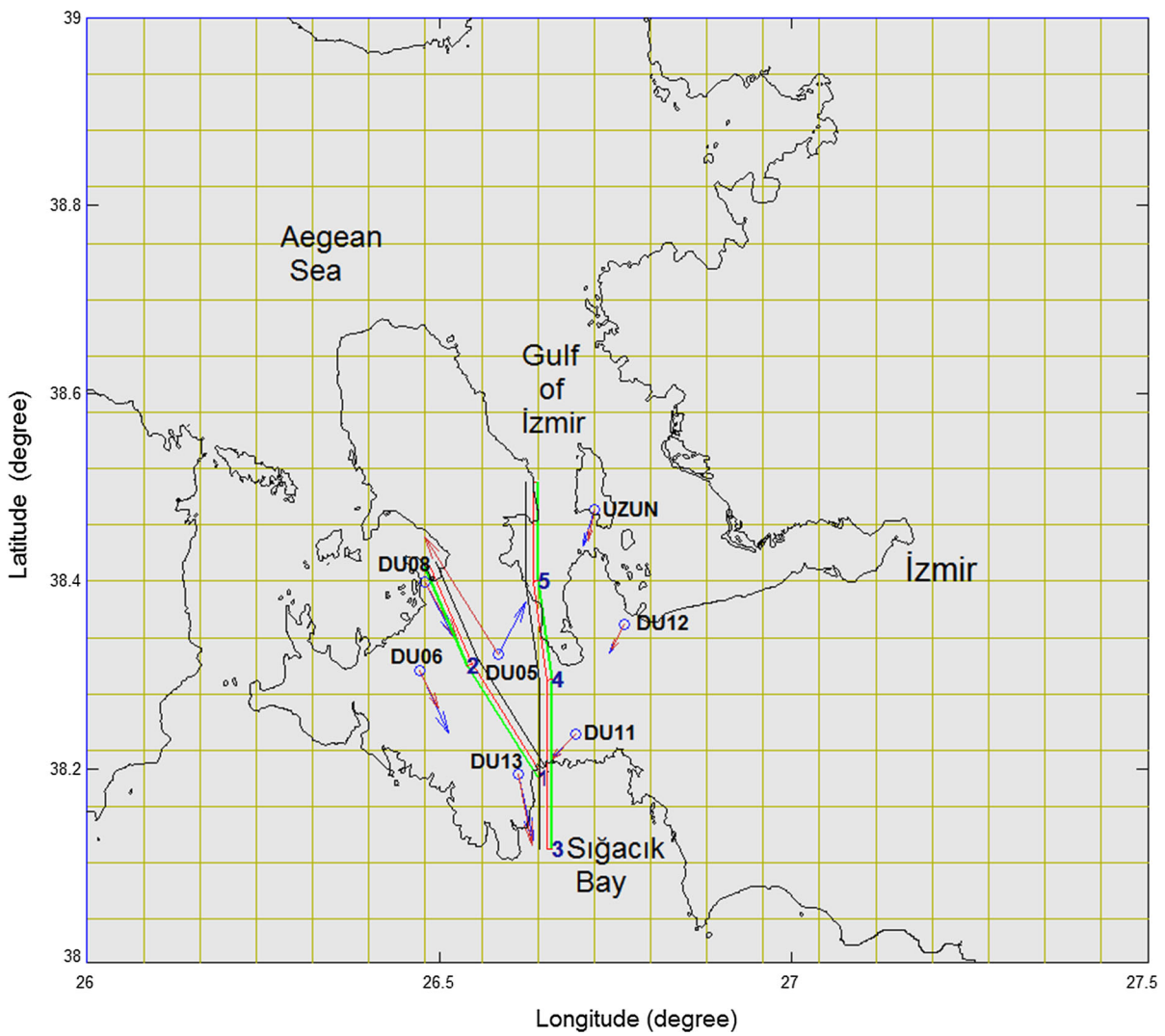

Figure 5
The model created using GNSS relative solutions of Gülbahçe fault and Uzunkuyu intrusive. *Blue vectors* represent the obtained GNSS velocities by GG and *red vectors* represent modelled GNSS velocities by Coulomb 3.3

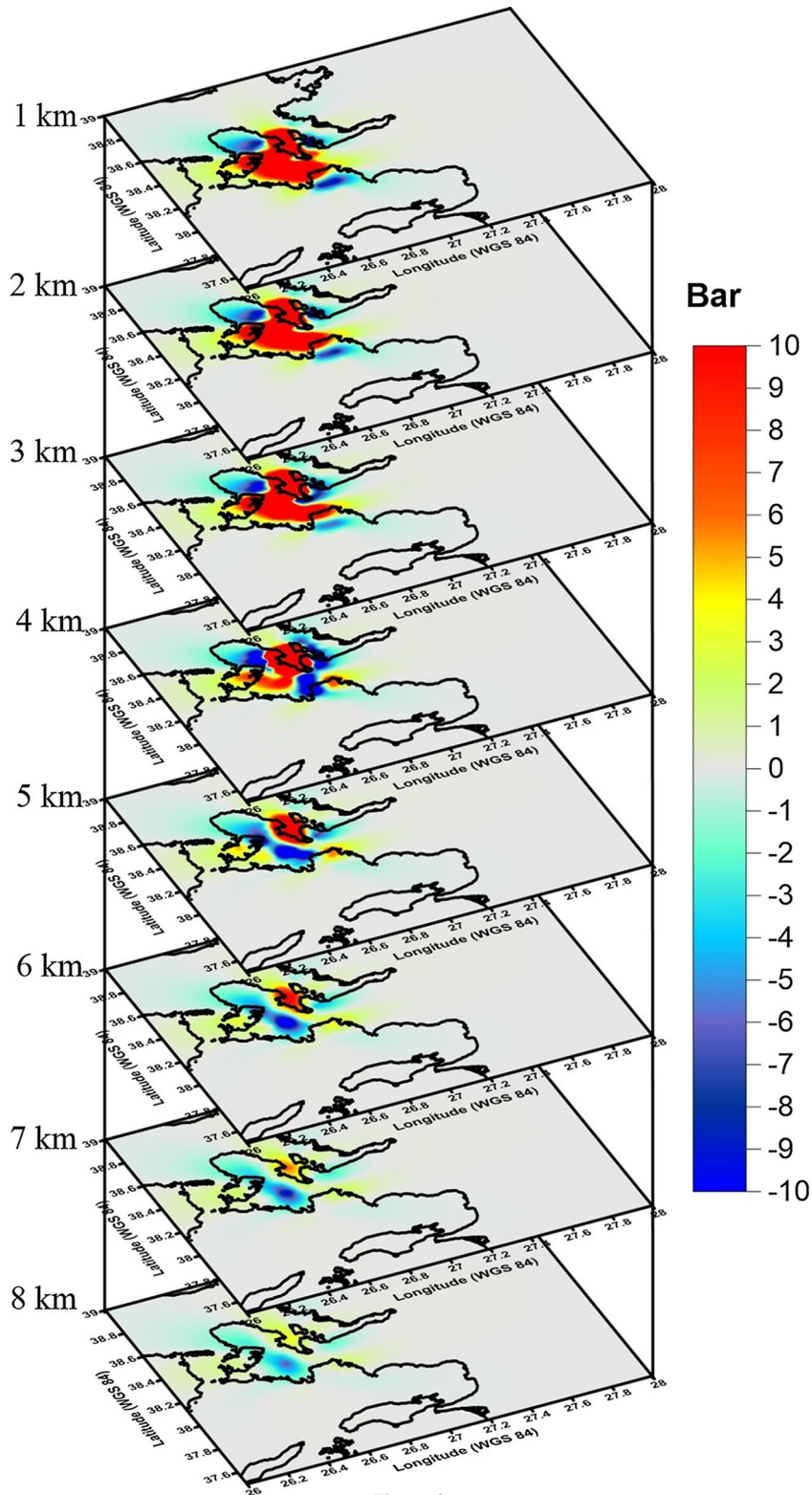

Figure 6
The Coulomb stress analysis maps of Uzunkuyu intrusive and Gülbahçe fault

that there are no significant changes in stress throughout the region at depths greater than 4 km. Therefore, the Coulomb strain was calculated for XX, YY and ZZ components (Figs. 7, 8, 9) and the strain dilations for 1 and 4 km were obtained (Fig. 10).

2.3. *Microgravity Analysis*

In this step, we performed the trend analysis for different orders (from 1st order to 20th order) to the Bouguer gravity anomalies obtained from TUBITAK project (Fig. 11). In that project, the gravity data were measured at each station with a minimum 60 s with five repetitive readings using Scintrex CG-5 Auto Grav Gravity device with sampling interval between 250 and 500 meters.

The trend surfaces help to generate suitable maps for separating the effects of deep and shallow sources in the gravity data. These are mathematical surfaces which represent a surface of best fit to the data points distributed in xyz-space. Such surfaces are defined by polynomial functions, and the surface is fit to the data points using least square methods (Burger 1992). Therefore, we tried to create various residual maps for different levels to obtain best consistency between main tectonic elements and gravity anomalies trend analysis.

The power spectrum is a method which is applied for examining the depth knowledge and the average square and the least error of variance are used for the spectrum prediction approximation. In this method, with the help of a window function, one dimensional data is separated into partitions and the spectrum is acquired for these partitions one by one. Therefore, the power spectrum is provided by calculating the arithmetic average of the values in distinct frequencies (Jenkis and Watts 1968). The power spectrum for each partition; $\bar{S}(w)$ and the number of the partitions; R are described as (Cianciara and Marcak 1976);

$$\bar{S}(w) = \frac{1}{R}\sum_{r=1}^{R}\sum_{p=1}^{P} f_r^p(w, \alpha_1^{pr}, \alpha_2^{pr}, \ldots \alpha_n^{pr}) \exp(-2wh), \quad (6)$$

Here, f is the anomaly function, α is parameters of the structure, h is the depth and w is the angular frequency. If the inversions in Eq. 6,

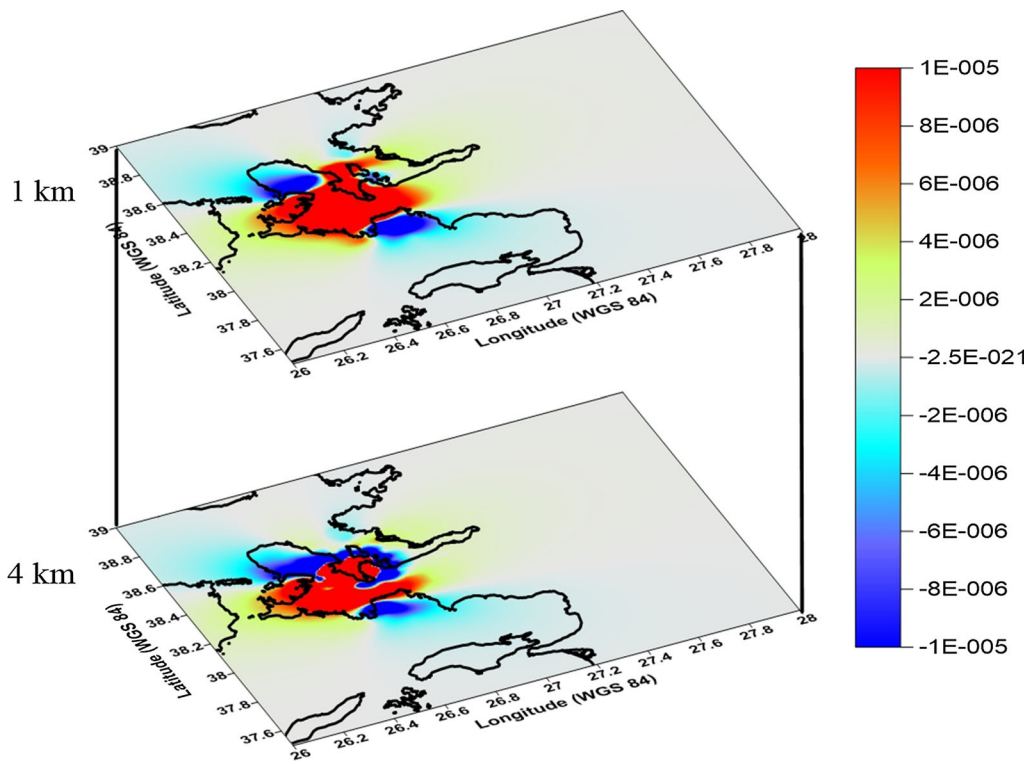

Figure 7
The Coulomb Strain XX-component maps of Uzunkuyu intrusive and Gülbahçe fault

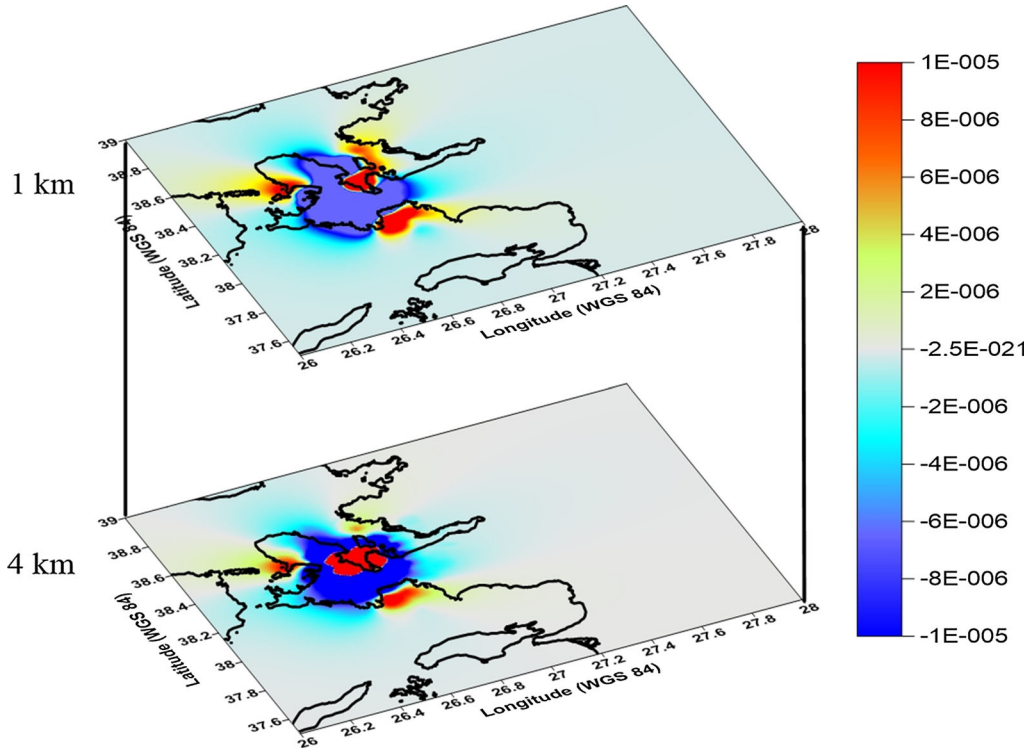

Figure 8
The Coulomb Strain YY-component maps of Uzunkuyu intrusive and Gülbahçe fault

$$f_r^p(w, \alpha_1^{pr}, \alpha_2^{pr}, \ldots, \alpha_n^{pr}) = c^{pr} = cons\tan t\, C = \sum_{r=1}^{R} \frac{1}{R} \sum_{p=1}^{P} c^{pr},$$

are calculated (Jenkins and Watts, 1968), Eq. (6) is formed as,

$$S = C.\exp(-2wh). \tag{7}$$

If the logarithm of Eq. (7) is taken, the mean depth of the structure is calculated by,

$$\bar{h}_i = \frac{\ln S(w_{i+1}) - \ln S(w_i)}{2(w_{i+1} - w_i)} \quad i = 1, 2, \ldots \tag{8}$$

3. Discussions

In GNSS relative solutions of Gülbahçe fault (Fig. 2), the motion of Gülbahçe fault is determined as right-lateral strike slip. Additionally, it is noticed that the area around DU13 is not affected by the mechanism of this fault (Fig. 2). In Coulomb modelling application for Gülbahçe fault (Fig. 4), it appears that the area around DU05 is partially affected by this fault.

In GNSS relative solutions of Uzunkuyu intrusive and its surrounding (Fig. 3), it is found that the motion of Uzunkuyu intrusive is left-lateral strike slip. Besides, although DU13 is also close to Gülbahçe fault, the area around this station is affected only by the kinematic structure of Uzunkuyu intrusive. Therefore, this result represents that Gülbahçe fault is not relevant for that region.

If the GNSS velocities given in Figs. 2 and 3 are evaluated together, it is seen that the amplitudes of velocities of Uzunkuyu intrusive are greater than those related to Gülbahçe fault.

When the Gülbahçe fault is modelled with Uzunkuyu intrusive by Coulomb modelling method (Fig. 5), it is noticed that GNSS solutions and model parameters are coherent with each other. It means that both tectonic structures are responsible for the movements of the study area. Therefore, DU05, which is located between Gülbahçe fault and

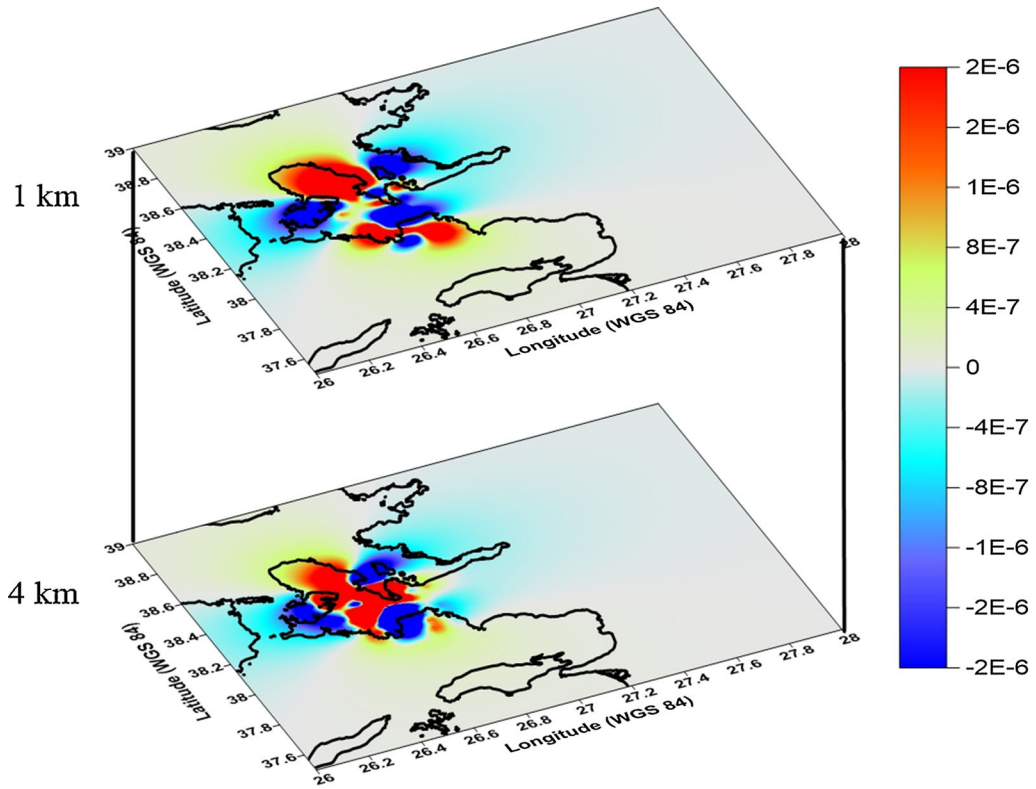

Figure 9
The Coulomb Strain ZZ-component maps of Uzunkuyu intrusive and Gülbahçe fault

Uzunkuyu intrusive, is affected by two different directional (right-lateral and left-lateral) mechanisms and also, it is thought that, there are structural problems in the area around DU05. The mechanism of this complicated area needs to be observed with GNSS station network including closely established stations.

In the stress change maps (Fig. 6) calculated for the depths between 1 km and 8 km, it is seen that Gülbahçe fault and Uzunkuyu intrusive create a combined kinematic structure whose effect is very marked at the depths between 1 and 4 km. It is noticed that the stress characteristics are maintained on submarine part of Uzunkuyu intrusive towards Chios Island (Fig. 1) in the depths between 1 and 4 km. The depth of 4 km of these tectonic structures is also verified by applying power spectrum to the gravity data. Additionally, at depths greater than 4 km, while the effect of tensional stress continue at north of Gülbahçe fault, the stress turns to compressional stress around Uzunkuyu intrusive (Fig. 6). It means that Uzunkuyu intrusive is affected by another mechanism at depths greater than 4 km.

When strain changes are examined (Figs. 7, 8) it is observed that the strain is characterized by extension in XX-component and compressive in YY-component. This result confirms the orientation of the faults as N–S. In ZZ-component and dilation maps (Figs. 9, 10) generally, the compressive-contraction kinematic is obtained in the study area except the area around Gülbahçe Bay. Gülbahçe bay has positive strain (tensile-extension features) in *X*–*Y*–*Z* directions. The tensile strain patterns in XX-component (Fig. 7) and in ZZ-component (Fig. 9) present similarities in some parts of the study area. This result shows that the tectonic structures act on both vertical and horizontal directions. According to the Coulomb dilation strain results (Fig. 10), we point out that while the part of Gülbahçe fault around the Izmir bay shows positive strain (tensile-extension kinematic) in ZZ-component, the

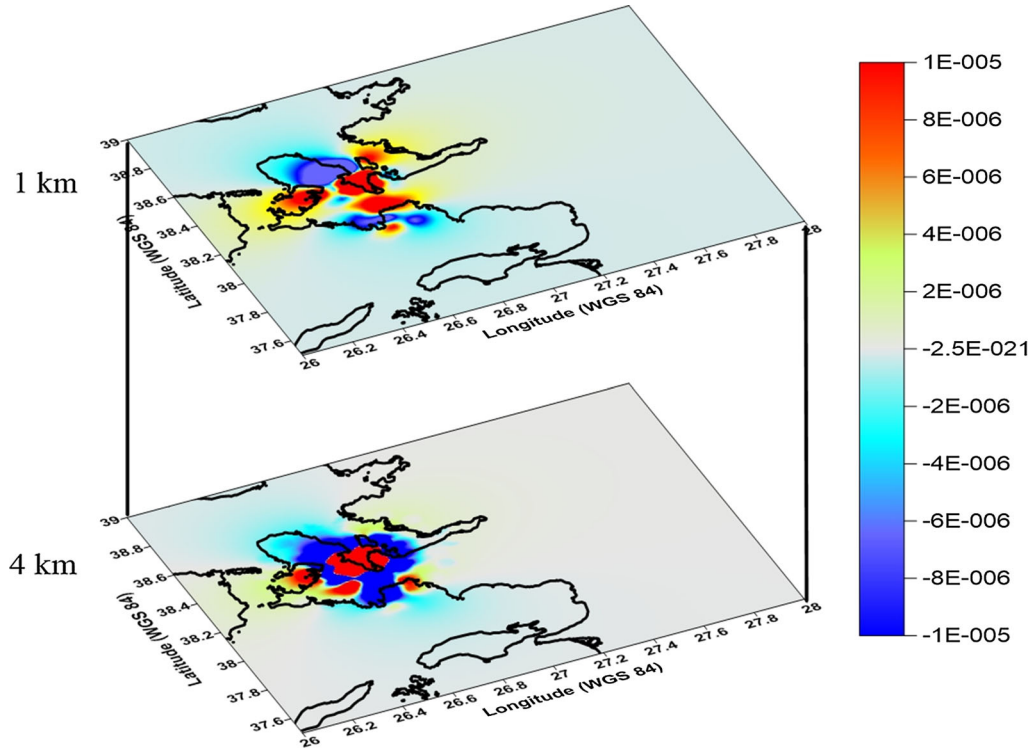

Figure 10
The Coulomb Strain dilatation maps of Uzunkuyu intrusive and Gülbahçe fault

compressive-contraction is observed in the part of fault near the northward part of Izmir bay which is called as the beginning of outer bay. The part of Gülbahçe fault towards outer of Izmir bay, where compressive mechanism in present, is explained by pushing effect from east to west obtained in the seismic interpretation of Ocakoglu et al. (2004). According to distributions of the ZZ-component strain and strain dilation (Figs. 9, 10), it is pointed out that the compression acts on XYZ plane.

In regard to the gravity results (Fig. 11), we note that Gülbahçe fault and Uzunkuyu intrusive effects are evident in the 1st order and 20th order trend maps. This means that these tectonic elements have both shallow and deep effects. However, Uzunkuyu intrusive is observed as dominant up to 10th trend. Therefore, it can be said that this element represents a regional feature. Particularly, the northern side of Gülbahçe fault, which shows greater residuals relative to Uzunkuyu intrusive, is seen more clearly in 12th trend and upwards.

Figure 11 ▶
Residual Bouguer gravity anomalies maps obtained by 1st–20th trend analysis and main tectonic structures of the study area (*all numbers* are indicated that the degree of trend analysis which subtracted from the Bouguer anomaly map to produce a residual map)

According to the Coulomb stress and strain analysis results, Uzunkuyu intrusive acts as a whole structure. However, based on the results of gravity and Coulomb stress and strain analysis, it is noticed that Gülbahçe fault has three different segments and the segment located near the Gülbahçe bay is more effective relative to the other components.

In the result of Coulomb modelling (Fig. 5), it is found that the senses of Uzunkuyu intrusive and Gülbahçe fault are pure strike-slip and reverse oblique, respectively. The differences on the fault senses are also seen on the gravity data. The gravity anomalies show that Uzunkuyu intrusive shows strike-slip fault character up to the 10th trend maps (Fig. 11). In the gravity anomalies along Gülbahçe

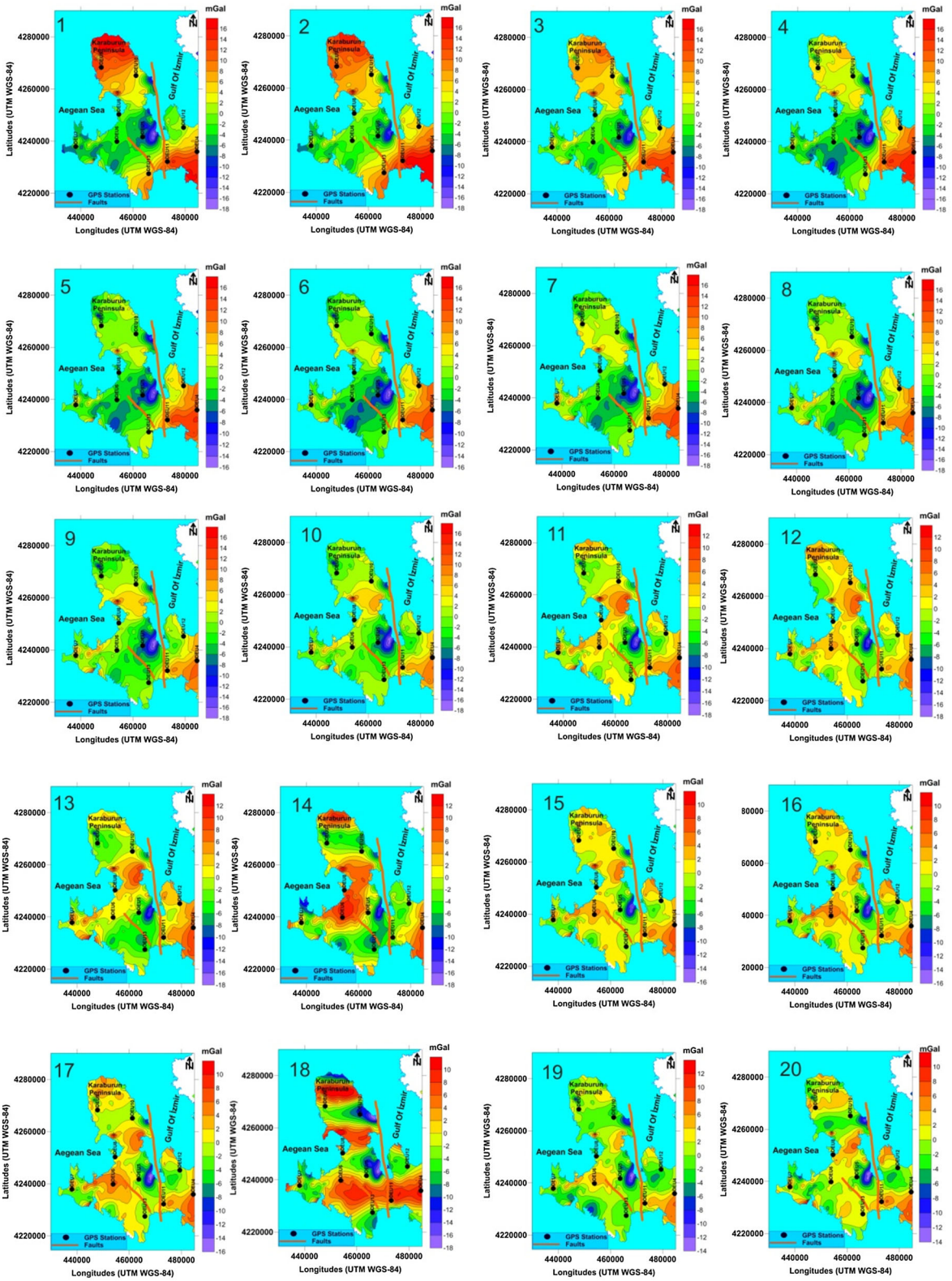
1
2
3
4
5
6
7
8
9
10
11
12
13
14
15
16
17
18
19
20
mGal
Karaburun Peninsula
Aegean Sea
Gulf Of Izmir
GPS Stations
Faults
Latitudes (UTM WGS-84)
Longitudes (UTM WGS-84)
4280000
4260000
4240000
4220000
440000
460000
480000

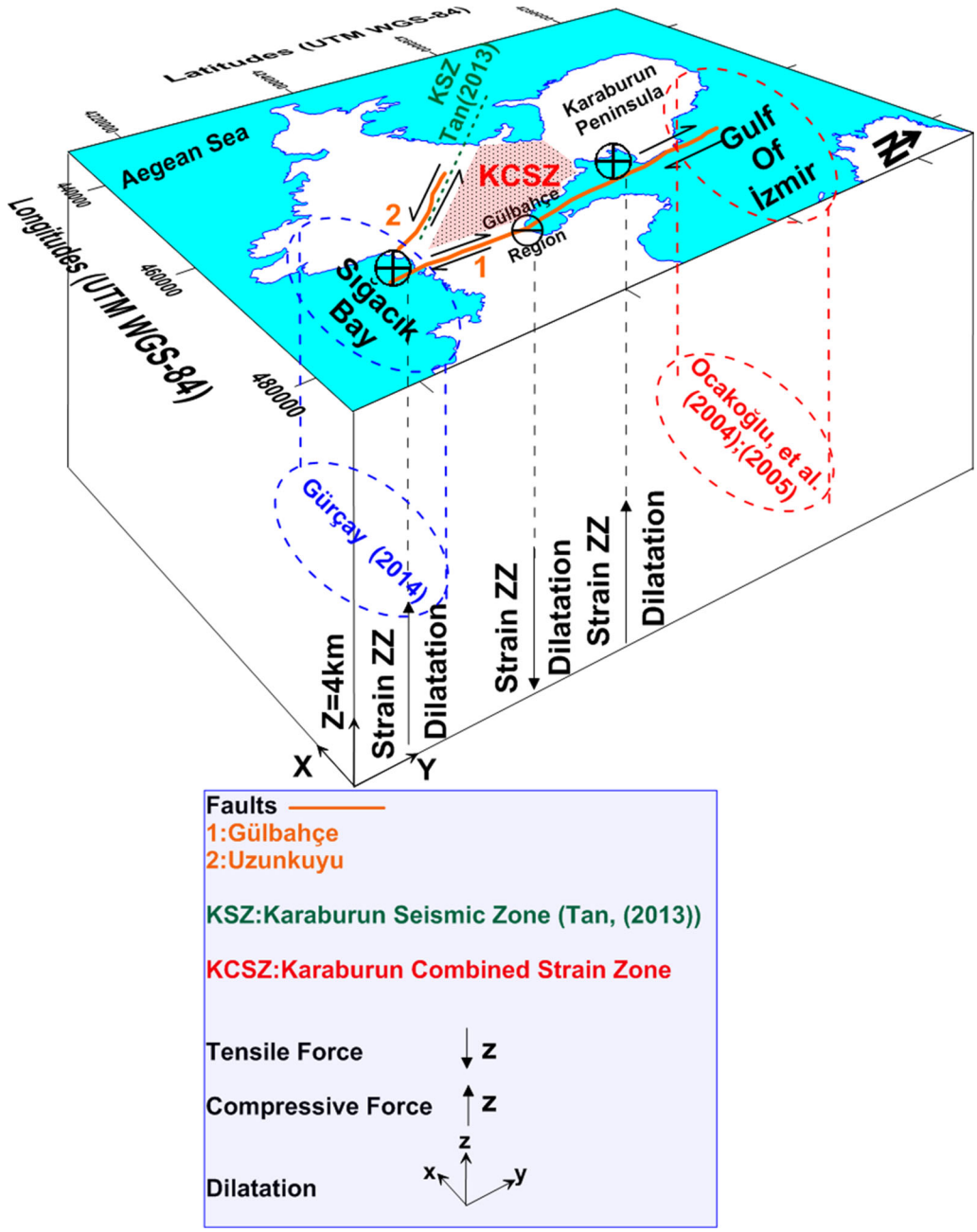

Figure 12
A scheme of the kinematics of the structures presented in the study area

fault, based on the non-symmetrical anomaly differences on two sides of the fault, indicates that the strike-slip fault includes a component. This case becomes more dominant on the north of Gülbahçe fault with high amplitude negative gravity anomalies (Fig. 11). These determinations are coherent with the results of previous geological and seismic studies (Emre et al. 2005).

The strain increases with increasing depth in the area located between Uzunkuyu intrusive and Gülbahçe fault mechanism (Fig. 10). These two different directional kinematic mechanisms create complicated

strain effects on DU5 and its surrounding, suggesting the need for detailed and gravity observation in this area.

Additionally, in the seismic study of Gürçay (2014) realized in Sığacık bay and its surrounding, it was pointed out that the sense of observed faults is strike-slip with compressive features and also, these faults represented uplifts which were defined as acoustic basement in some parts of Sığacık bay and its surrounding.

Consequently, we defined a schematic description of the geodynamic model of the region (Fig. 12) and the compressive stress is seen in Sığacık bay and tensile stress is seen in Gülbahçe bay. In other words, while a continental contraction (shortening) is shown in Sığacık bay, extension occurs in Gülbahçe bay (Figs. 9, 10).

Acknowledgements

This study has been carried out within the project No. 108Y285, The Scientific and Technological Research Council of Turkey (TUBITAK). We would like to thank editor-in-chef Prof. Dr. Carla F. Braitenberg and the anonymous reviewers for their constructive suggestions.

References

Aksu, A. E., Piper, D. J. W., & Konuk, T. (1987). Late Quaternary tectonic and sedimentary history of outer Izmir and Candarli Bays, Western Turkey. *Marine Geology, 76,* 89–104.

Altunkaynak, S., & Yilmaz, Y. (2000). Geology and active tectonic of foça area, Western Anatolia. In: *BADSEM 2000 symphony* (pp. 160–165). Izmir.

Barka, A.A., (1992). The North Anatolian fault zone, *Annales Tectonicae, VI*, 164–195.

Bozkurt, E. (2001). Neotectonics of Turkey—a synthesis. *Geodinamica Acta, 14,* 3–30.

Burger, H.R. (1992). Exploration geophysics of the shallow subsurface, Prentice Hall.

Cianciara, B., & Marcak, H. (1976). Interpretation of gravity anomalies by means of local power spectra. *Geophysical Prospecting, 24*(2), 273–286.

Dewey, J. F., & Şengör, A. C. (1979). Aegean and surrounding regions: complex multiplate and continuum tectonics in a convergent zone. *Geological Society of America Bulletin, 90*(1), 84–92.

Emre, O., & Barka, A. (2000). Active faults between Gediz Graben and Aegean Sea (Izmir Region). In: BADSEM 2000 Symposium Abstract Book, Izmir, Turkey, 24–27 May 2000.

Emre, O., Ozalp, S., Doğan, A., Ozaksoy, V., Yıldırım, C., Goktaş, F. (2005). *İzmir Yakın Çevresinin Diri Fayları ve Deprem Potansiyelleri [The Active Faults of the İzmir Region and Their Earthquake Potentials]*. Mineral Research and Exploration Institute of Turkey (MTA) Report no. 10754 **(in Turkish, unpublished)**.

Genç, C., Altunkaynak, S., Karacık, Z., Yazman, M., & Yılmaz, Y. (2001). The Çubukludağ graben, south of Izmir: tectonic significance in the Neogene geological evolution of the Western Anatolia. *Geodinamica Acta, 14,* 1–12.

Gürçay, S. (2014). Investigation of submarine active tectonism of the Gulf of Sığacık and Surroundings by high resolution seismic methods, Ph.D. Thesis, Dokuz Eylul University, The Graduate School of Natural and Applied Sciences, Izmir, Turkey.

Herring, T. A., King, R.W., McClusky, S.C. (2010a). GAMIT reference manual: GPS analysis at MIT, Release 10.4: MIT, Cambridge.

Herring, T. A., King, R.W., and McClusky, S.C. (2010b). GLOBK global Kalman filter VLBI and GPS analysis program, Release 10.4: MIT, Cambridge.

Jenkins, G. M., & Watts, D. G. (1968). *Spectral analysis and its applications*. San Francisco: Holden-Day.

Kaya, O. (1979). The stratigraphy and tectonics of the Middle Eastern Aegean depression. *Bulletin Geological Society Turkey, 22,* 35–58.

Kaya, O. (1981). Miocene reference section for the coastal parts of West Anatolia. *Newsletters on Stratigraphy, 10,* 164–191.

Kaymakcı, N., Aldanmaz, E., Langereis, C., Spell, T. L., Gurer, O. F., & Zanetti, K. A. (2007). Late Miocene transcurrent tectonics in NW Turkey: evidence from palaeomagnetism and 40Ar–39Ar dating of alkaline volcanic rocks. *Geological Magazine, 144,* 379–392.

King, R.W., & Bock, Y. (2009). Documentation for the GAMIT analysis software, Release 10.3: MIT, Cambridge.

King, G. C. P., Stein, R. S., & Lin, J. (1994). Static stress changes and the triggering of earthquakes. *Bulletin Seismology Society America, 84,* 935–953.

Kocyiğit, A., & Özacar, A. A. (2003). Extensional neotectonic regime through the NE edge of the Outer Isparta Angle, SW Turkey: new field and seismic data. *Turkish Journal of Earth Science, 12,* 67–90.

Lin, J., & Stein, R. S. (2004). Stress triggering in thrust and subduction earthquakes and stress interaction between the southern San Andreas and nearby thrust and strike-slip faults. *Journal Geophysical Research, 109,* B02303. doi:10.1029/2003JB002607.

McKenzie, D. (1972). Active tectonics of the mediterranean region. *Geophysical Journal International, 30*(2), 109–185

Ocakoğlu, N., Demirağ, E., & Kuşçu, I. (2004). Neotectonic structures in the area offshore of Alaçatı. *Doğanbey and Kuşadası, western Turkey: Evidence of strike-slip faulting in the Aegean extensional province, Tectonophysics, 391,* 67–83.

Ocakoğlu, N., Demirağ, E., & Kuşçu, I. (2005). Neotectonic structures in Izmir Gulf and surrounding regions (westernTurkey): evidences of strike-slip faulting with compression in the Aegean extensional regime. *Marine Geology, 219,* 155–171.

Pamukçu, O., Gönenç, T., Çırmık, Y. A., & Kahveci, M. (2015a). Investigation of the Sığacık Bay's Displacement Characteristic by using GPS and gravity data in Western Anatolia. *Journal of Asian Earth Sciences, 99,* 72–84.

Pamukçu, O., Gönenç, T., Çırmık, A., Sındırgı, P., Kaftan, İ., & Akdemir, Ö. (2015b). Investigation of vertical mass changes in the south of Izmir (Turkey) by monitoring microgravity and GPS/GNSS methods. *Journal of Earth System Science, 124,* 137–148.

Pamukçu, O., Gönenç, T., Uyanik, O., Sözbilir, H., & Çakmak, O. (2014). A microgravity model for the city of İzmir (Western Anatolia) and its tectonic implementations. *Acta Geophysica, 62*(4), 849–871.

Saroglu, F., Emre, O. and Kuscu, I. (1992). Active Fault Map of Turkey, General Directorate of Mineral Research and Exploration MTA, Eskisehir Yolu, 06520, Ankara, Turkey

Şengor, A.M.C., Görür, N. and Şaroğlu, F. (1985). Strike-slip faulting and related basin formation in zones of tectonic escape: Turkey as a case study. *In*: Biddle, K. and Chrıstie-Blick, N. (eds), Strike-Slip Deformation, Basin Formation and Sedimentation. *Soc. Eco. Paleontologists Mineralogists*, Special Publications, 37, 227–264.

Tan, O. (2013). The dense micro-earthquake activity at the boundary between the Anatolian and South Aegean microplates. *Journal of Geodynamics, 65*(2013), 199–217.

Taymaz, T., Yılmaz, Y., & Dilek, Y. (2007). The geodynamics of the Aegean and Anatolia: Introduction. *In:* Taymaz, T., Yılmaz, Y., & Dilek, Y. (eds), *The Geodynamics of the Aegean and Anatolia*. (vol. 291, pp. 1–16). London: Geological Society, Special Publications.

Toda, S., Stein, R.S., Richards-Dinger K., & Bozkurt, S.B. (2005). Forecasting the evolution of seismicity in southern California: Animations built on earthquake stress transfer. *Journal Geophysics Research, 110*, B05S16. doi:10.1029/2004JB003415.

Uzel, B., Langereis, C. G., Kaymakci, N., Sözbilir, H., Özkaymak, Ç., & Özkaptan, M. (2015). Paleomagnetic evidence for an inverse rotation history of Western Anatolia during the exhumation of Menderes core complex. *Earth Planet Science Letter, 414,* 108–125.

Uzel, B., & Sözbilir, H. (2008). A first record of strike-slip basin in western Anatolia and its tectonic implication: the Cumaovası basin as an example. *Turkish Journal Earth Science, 17,* 559–591.

Uzel, B., Sözbilir, H., & Özkaymak, Ç. (2012). Neotectonic evolution of an actively growing superimposed basin in western Anatolia: the inner bay of İzmir, Turkey. *Turkish Journal Earth Science, 21*(4), 439–471.

(Received June 22, 2016, revised December 21, 2016, accepted January 15, 2017, Published online February 2, 2017)